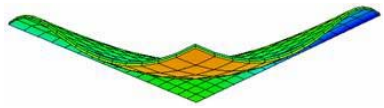

© 2004, The First International Conference on Computational Mechanics (CM'04)
Belgrade, Serbia and Montenegro, November 15-17, 2004
http://www.cm2004.matf.bg.ac.yu
Printing Faculty of Mathematics, University of Belgrade

Modelling of Ductile Failure in Metals under High Velocity Impact Loading

A. A. Lukyanov, R. Vignjevic♣, V. Panov, N. Bourne

Crashworthiness, Impact and Structural Mechanics (CISM),
School of Engineering, Cranfield University, Cranfield,
Bedford MK43 OAL, UK

e-mail♣: v.rade@cranfield.ac.uk

Abstract The objective of the work presented in this paper was to generate the thermodynamically consistent coupled thermo-elastic-plastic damage model of solid media at a macroscopic level applicable to hypervelocity impacts. The model is based on the thermodynamics of irreversible processes and the assumption that damage within a continuum can be represented as a damage tensor ω_{ij} [1], [4]. This allows for definition of two scalars that are $\omega = \omega_{kk}/3$ (the volume damage) [2], [3] and $\alpha = \sqrt{\omega'_{ij}\omega'_{ij}}$ (a norm of the damage tensor deviator $\omega'_{ij} = \omega_{ij} - \omega\delta_{ij}$) [4]. The parameter ω describes the accumulation of micro-pore type damage (which may disappear under compression) and the parameter α describes the shear related damage. The parameter ω may be considered as a volume content of micro-pores in the material. In the damage-free material we have $\omega = \alpha = 0$; if damage is accumulated, ω and α increase in such a manner that they remain less than one. This damage evolution is then coupled to a strain, strain-rate and temperature dependent plasticity model. The initiation of failure is based on a critical value of a specific dissipation function. The performance of the model in modelling high velocity impacts is illustrated by few numerical examples.

Keywords: damage, ductile failure, irreversible thermodynamics, dissipation.

1. Introduction

Thermo-mechanical processes which occur in deformable solids under intensive dynamic loading consist of coupled mechanical, thermal and structural stages. The structural processes involve the formation, motion and interaction of defects in metallic crystals, phase transitions, breaking of bonds between molecules, accumulation of micro-structural damages (pores, cracks), etc. Irreversible deformations, zones of adiabatic shear and micro-fracture are caused by these processes. Dynamic fracture is a complicated multistage process which includes the initiation, evolution and coalescence of micro-defects (damage) and cracks.

The development of fracture mechanics originated in the papers of Kachanov [2] and Rabotnov [3], dealing with theory of creeping of materials, where one scalar damage parameter was introduced. Some time later, Ilyushin [1] proposed tensor damage. Attempts to introduce these tensors are currently being considered [4], [5-7]. The introduction of the damage parameters into the system of internal variables and the use of thermodynamic principles of continuum mechanics allows the construction of thermodynamically-correct coupled models of solids with damage Coleman [4] and [6, 7].

The model presented in this paper is constructed within the framework of continuum damage mechanics is used to describe the initiation and evolution of damage under impact loadings. The damage growth ultimately results in the initiation of macro-cracks. The model for ductile fracture is intended for isentropic damage conditions including the commonly observed stages of ductile fracture:
The formation of voids
The growth of voids due to plastic straining and hydrostatic stress
The coalescence of growing voids leading to fracture

♣ Corresponding author

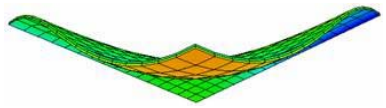

© 2004, The First International Conference on Computational Mechanics (CM'04)
Belgrade, Serbia and Montenegro, November 15-17, 2004
http://www.cm2004.matf.bg.ac.yu
Printing Faculty of Mathematics, University of Belgrade

The model allows for spherical and ellipsoidal microvoids whose size, shape and orientation can evolve. The thermodynamic potential is a quadratic, that can also be used to define a yield function, in which the MTS model is used to define flow stress.

2. Basic Thermodynamics Assumptions

The basic premise of the theory of a thermo-elastic-plastic medium with damage is that the state of material at any point within continuum is fully determined by:

The elastic and plastic parts of the full strain tensor, i.e. the rate of deformation is can be divided into elastic and plastic parts: $\dot{\tilde{\varepsilon}} = \dot{\tilde{\varepsilon}}^{p} + \dot{\tilde{\varepsilon}}^{e}$, plastic rate of deformation is regarded as incompressible $\dot{\varepsilon}^{p}_{kk} = 0$ as it is in the basic theory of plasticity and elastic strains are assumed small: $\tilde{\varepsilon}^{e} : \tilde{\varepsilon}^{e} << 1$.

The temperature or entropy s, (Where $ds = ds_e + ds_i$, ds_e - is the differential of external entropy, ds_i - is the differential of internal entropy which describes the irreversibility of deformation), Damage parameters ω and α, which describe the void growth in solids, $\Re$ which characterize the extent of work hardening.

Further, the derivation is done using Lagrange's (material) coordinates. Besides, it is assumed that the system meets conservation laws of mass and momentum. Having in mind that the objective is modeling of high velocity impacts a further assumption is made that the deformation process is adiabatic and consequently there is neither heat exchange nor heat source within the material.

Using Lagrange's coordinate system regarding current configuration the first law of thermodynamics (conservation of energy equation) in differential form is:

$$\rho \frac{\partial U}{\partial t} = \tilde{\Sigma} : \frac{\partial \tilde{\varepsilon}}{\partial t} - \nabla \cdot \vec{q} \tag{1}$$

Normally, parameters s_e, s_i have the following definition:

$$\frac{\partial s_e}{\partial t} = -\frac{1}{\rho} \nabla \cdot \vec{S}, \quad \rho \frac{\partial s_i}{\partial t} = d = \sum X_\alpha \chi_\alpha \geq 0 \tag{2}$$

The second law of thermodynamics could be expressed in the form of Clausius-Duhem inequality:

$$\frac{\partial s}{\partial t} \geq -\frac{1}{\rho} \nabla \cdot \vec{S}, \quad \vec{S} = \frac{\vec{q}}{T}. \tag{3}$$

On introducing free energy $F = U - Ts$ in place of internal energy U Equation (1) could be rewritten in the following form:

$$0 = \frac{1}{\rho} \tilde{\Sigma} : \frac{\partial \tilde{\varepsilon}}{\partial t} - \frac{1}{\rho} \nabla \cdot \vec{q} - \dot{T}s - T\dot{s} - \dot{F} \tag{4}$$

The inequality Equation (3), using Equation (4) takes the form:

$$\frac{1}{\rho} \tilde{\Sigma} : \frac{\partial \tilde{\varepsilon}}{\partial t} - \frac{1}{\rho} \frac{\vec{q} \cdot \nabla T}{T} - \dot{T}s - \dot{F} \geq 0 \tag{5}$$

The free energy being the function of state parameters $F = F(\tilde{\varepsilon}^{e}, \tilde{\varepsilon}^{p}, T, \omega, \alpha, \Re)$, $\dot{\tilde{\varepsilon}} = \dot{\tilde{\varepsilon}}^{e} + \dot{\tilde{\varepsilon}}^{p}$, the inequality Equation (5) yields the following condition valid for all the processes taking place within the continuum:

$$\left(\frac{1}{\rho}\tilde{\Sigma} - \frac{\partial F}{\partial \tilde{\varepsilon}^{e}}\right) : \dot{\tilde{\varepsilon}}^{e} + \left(\frac{1}{\rho}\tilde{\Sigma} - \frac{\partial F}{\partial \tilde{\varepsilon}^{p}}\right) : \dot{\tilde{\varepsilon}}^{p} - \left(\frac{\partial F}{\partial T} + s\right)\dot{T} - \frac{\partial F}{\partial \omega}\dot{\omega} - \frac{\partial F}{\partial \alpha}\dot{\alpha} - \frac{\partial F}{\partial \Re}\dot{\Re} - -\frac{1}{\rho}\frac{\vec{q} \cdot grad\, T}{T} \geq 0 \tag{6}$$

It follows from Equation (6) that:

$$\tilde{\Sigma} = \rho \frac{\partial F}{\partial \tilde{\varepsilon}^{e}} \tag{7}$$

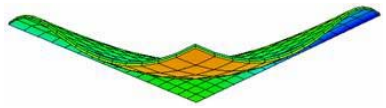

Belgrade, Serbia and Montenegro, November 15-17, 2004
http://www.cm2004.matf.bg.ac.yu
Printing Faculty of Mathematics, University of Belgrade

$$s = -\frac{\partial F}{\partial T}$$

Using Equation (7) the inequality Equation (6) can be transformed as follows:

$$d = d_M + d_F + d_T \geq 0 \tag{8}$$

Where:

$$d_M = \underbrace{\frac{1}{T}\left(\tilde{\Sigma} - \rho\frac{\partial F}{\partial \tilde{\varepsilon}^p}\right) : \dot{\tilde{\varepsilon}}^p}_{d_M^1} \underbrace{- \rho\frac{\partial F}{\partial \Re}\dot{\Re}}_{d_M^2}$$

$$d_T = -\frac{\vec{q} \cdot grad\, T}{T^2} \tag{9}$$

$$d_F = -\frac{\rho}{T}\frac{\partial F}{\partial \omega}\dot{\omega} - \frac{\rho}{T}\frac{\partial F}{\partial \alpha}\dot{\alpha}$$

Equations (9) show that the accumulation of dissipation process is governed not by actual stresses $\tilde{\Sigma}$, but by the dissipation contributing stress defined by the expression in brackets. The dependency of F on plastic deformation $\tilde{\varepsilon}^p$, allows for the strain anisotropy of the material to be taken into account in plastic deformation.

Making use of Equation (9) and $F = U - Ts$ Equation (1) could be written in the following form:

$$\rho\dot{s} = d_M + d_F - \nabla \cdot \vec{q} \tag{10}$$

The general equations developed above are applied to modeling damage in metals by making the following assumptions:

1. Elastic strains are small: $\tilde{\varepsilon}^e : \tilde{\varepsilon}^e << 1$
2. The dissipation function Equation (8) is a sum of three non-negative terms defined by Equations (9):

$$d_M \geq 0, d_F \geq 0, d_T \geq 0 \tag{11}$$

According to Duhamel's law for heat conductivity $\vec{q} = -\boldsymbol{\kappa} \cdot grad\, T$ thermal dissipation is non-negative, i.e.:

$$d_T = \frac{grad\, T \cdot \boldsymbol{\kappa} \cdot grad\, T}{T} \geq 0 \tag{12}$$

Where: $\kappa > 0$ -is a symmetrical heat conductivity tensor (positive semidefinite).

The hypothesis $d_M^1 \geq 0$ - is easy to proof using Clausius - Plank's inequality. $\tilde{\Sigma} : \dot{\tilde{\varepsilon}}^p - \dot{F} - s\dot{T} \geq 0$.

3. For dissipation due to development of damage and fracturing the following equations of state are assumed:

$$-\rho\frac{\partial F}{\partial \omega} = \Lambda_1\dot{\omega}$$

$$-\rho\frac{\partial F}{\partial \alpha} = \Lambda_2\dot{\alpha} \tag{13}$$

$$Q = \hat{Q}\left(\left|\tilde{\Re}\right|, T, \Re\right) = -\rho\frac{\partial F}{\partial \Re} = \Lambda_3\dot{\Re}$$

The relationship Equation (13) establishes a linear functional dependence between the thermodynamic force and thermodynamic flux in accordance with Onsager theory. Therefore, dissipation due to damage and fracture is non-negative $d_F \geq 0$ and dissipation due to of work hardening $d_M^2 \geq 0$.

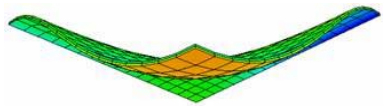

© 2004, The First International Conference on Computational Mechanics (CM'04)
Belgrade, Serbia and Montenegro, November 15-17, 2004
http://www.cm2004.matf.bg.ac.yu
Printing Faculty of Mathematics, University of Belgrade

4. The free energy of the medium could be presented in the form of a sum of two terms:

$$F = F_1(\tilde{\varepsilon}^e, T) + F_2(\tilde{\varepsilon}^p, T) \tag{14}$$

The first equation of state in Equations (7) combined with Equations (13) is equivalent to an assumption that accumulated plastic deformation does not lead to any variations of elastic properties of the material.

Furthermore, the following relationship:

$$-\rho \frac{\partial F}{\partial \tilde{\varepsilon}^p} = \Gamma \tilde{\varepsilon}^p \tag{15}$$

is assumed, where $\Gamma \geq 0$ is the parameter for material strain anisotropy, which characterizes the strain anisotropy which develops due to the plastic deformation.

5. It is assumed that all thermodynamic potentials U, F and S contain one term that depends only on temperature, for example:

$$F(T, \tilde{\mu}_i) = F_0(T) + \hat{F}(T, \tilde{\mu}_i) \tag{16}$$

6. For free energy it is assumed that

$$\frac{\partial \hat{F}}{\partial T} = -\frac{1}{\rho}[\alpha_v \cdot \Sigma] \tag{17}$$

7. Elastic parameter Lame λ, shear modulus μ, dynamic viscosity η, yield stress Y are functions of the damage parameters ω, α :

$$\lambda = \lambda_0(1-\omega)(1-\alpha), \mu = \mu_0(1-\omega)(1-\alpha), \eta = \eta_0(1-\omega)(1-\alpha), \; Y = Y_0(1-\omega)(1-\alpha) \tag{18}$$

Where: K_0, μ_0, η_0, Y_0 are material parameters in an undamaged state.

8. The kinetic (evolution) equations for ω and α have the following form [4], [5]:

$$\dot{\omega} = \varphi(\omega, \alpha, \Sigma) = B\left(\frac{\Sigma}{(1-\omega)(1-\alpha)} - \Sigma_*\right) H\left(\frac{\Sigma}{(1-\omega)(1-\alpha)} - \Sigma_*\right) +$$

$$+ \omega \frac{\Sigma - \Sigma^+}{4\eta_0} H\left(\Sigma - \Sigma^+\right) + \omega \frac{\Sigma - \Sigma^-}{4\eta_0} H\left(\Sigma^- - \Sigma\right), \; \Sigma^+ = -\frac{2}{3} Y_0 \ln \omega, \Sigma^- = -\Sigma^+ \tag{19}$$

$$\dot{\alpha} = \psi(\omega, \alpha, \Re_u) = C\left(\frac{\Re_u}{(1-\omega)(1-\alpha)} - \Re_u^*\right) H\left(\frac{\Re_u}{(1-\omega)(1-\alpha)} - \Re_u^*\right) \tag{20}$$

The kinetic equation for the volume damage ω consists of three terms. The first one has the form of the Tuler – Bucher equation [9] and describes the initiation and growth of the volume damage ω. The second term takes into account the viscous void growth in tension, while the third term describes the viscoplastic flow in compression see Kiselev, Lukyanov [4].

3. Constitutive Assumptions

The behaviour of materials under general three-dimensional stress states is usually simulated by decomposing the stress into hydrostatic components (pressure term) and deviatoric components. The two formulations are taken to be independent of each other since plastic flow is considered to be independent of pressure at low pressures for fully dense metals. At very high pressures, some attempts have been made to incorporate pressure dependence into the yield criterion [10].

From the continuum point of view simplest model of rate-dependence plasticity requires the specification of rate of plastic deformation, thermodynamic force according to the hardening parameter and rate of work hardening:

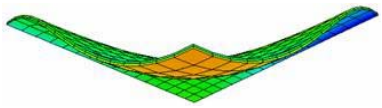

© 2004, The First International Conference on Computational Mechanics (CM'04)
Belgrade, Serbia and Montenegro, November 15-17, 2004
http://www.cm2004.matf.bg.ac.yu
Printing Faculty of Mathematics, University of Belgrade

$$Q = \hat{Q}\left(\left|\tilde{\Re}\right|, T, \Re\right) = -\rho \frac{\partial F}{\partial \Re} = \Lambda_3 \dot{\Re} \tag{23}$$

$$\dot{\tilde{\varepsilon}}^p = \Im\left(\left|\tilde{\Re}\right|, T, \Re\right) \frac{\tilde{\Re}}{\left|\tilde{\Re}\right|} \tag{24}$$

$$\dot{\Re} = \xi\left(\left|\tilde{\Re}\right|, T, \Re\right) \tag{25}$$

In the literature of adiabatic shearing and plasticity see Wright [11], the usual practice is to specify a flow rule corresponding to the Equation (24) and a work hardening relation corresponding to the Equation (25), but to ignore the specification of the thermodynamic force $\hat{Q}\left(\left|\tilde{\Re}\right|, T, \Re\right)$. In this work we take into account the thermodynamic force which is described through the Onsager theory by the Equation (23). Equations (23) and (25) give contribution to the system of constitutive equation as it will be shown further.

Mathematical models for effect of temperature and strain rate generally fall into one of two categories. Either the modelling is strictly empirical and intended only to capture dominant effects over a limited range of variables, or it is based on arguments from more or less elementary dislocation dynamics and then calibrated by choosing unknown parameters so as to fit selected data.

3.1 Description of Mechanical Threshold Stress (MTS) model

MTS stands for mechanical threshold stress (see 11-13]) and refers to internal variable (or variables) that evolves as plastic deformation progresses. The basic idea is the same as that used by Zerilli and Armstrong, that the stress required to move a single dislocation past an obstacle is composed of both thermal and athermal components. The strain rate for the thermal component obeys an Arrhenius law. The flow stress can be written in the following form:

$$\left(\left|\tilde{\Re}\right| - \Re_a\right)^m = \sum_{i=1}^{n} \left[f_i(\dot{\gamma}^p, T) \hat{f}_i\right]^m \tag{26}$$

where n is number of different types of impediments to the motion of dislocation, and the power m is chosen empirically, $1 \le m \le 2$. The term $\Re_a$ is called an athermal stress and may be either a constant or an evolution internal variable, and the $\hat{f}_i$ are called structural variables that also evolve as deformation progresses, $f_i(\dot{\gamma}^p, T)$.

In this paper the following flow stress is considered:

$$\frac{\Re}{\mu} = \frac{\Re_a}{\mu} + f_1(\dot{\varepsilon}, T) \frac{\hat{f}_1}{\mu_0} \tag{27}$$

where μ is shear modulus, μ_0 is shear modulus at the reference temperature, $f_1(\dot{\varepsilon}, T)$ is thermal activation function. Function $\hat{f}_1$ evolves with strain and can be described as following relation:

$$\frac{d\hat{f}_1}{d\varepsilon} = \theta_0 - \theta_r(T, \dot{\varepsilon}, \hat{f}_1) \tag{28}$$

where θ_0 is hardening (initial) due to dislocation accumulation, θ_r is the dynamic recovery rate. Assumption that rate of hardening decreasing with increasing deformation is assumed and Equation (27) can be written in the following form:

$$\frac{d\hat{f}_1}{d\varepsilon} = \theta_0 \left[1 - F(\hat{f}_1)\right] \tag{29}$$

where $F(\hat{f})$ is empirically derived dynamic recovery rate. To complete system of equation which is described flow stress several function of $F(\hat{f})$ was suggested. One of the expression can be written in the following rule:

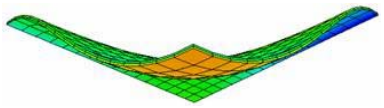

© 2004, The First International Conference on Computational Mechanics (CM'04)
Belgrade, Serbia and Montenegro, November 15-17, 2004
http://www.cm2004.matf.bg.ac.yu
Printing Faculty of Mathematics, University of Belgrade

$$F(\hat{f}_1) = \left(\frac{\tanh\left[\alpha \frac{\hat{f}_1}{\hat{f}_{es}(\dot{\varepsilon}, T)} \right]}{\tanh(\alpha)} \right) \tag{30}$$

where α is an empirical best-fit constant which dictates the rate at which saturation is achieved, $\hat{f}_{es}$ is temperature and rate-sensitive saturation stress, $\hat{f}_1$ represents flow stress contribution. Relationships for initial strain hardening rate θ_0 and saturation threshold stress $\hat{f}_{es}$ can be expressed as follows:

$$\theta_0 = a_0 + a_1 \ln(\dot{\varepsilon}) + a_2 \dot{\varepsilon}^n \tag{31}$$

$$\hat{f}_{es} = \hat{f}_{es}^0 \left(\frac{\dot{\varepsilon}}{\dot{\varepsilon}_{es}^0} \right)^{\frac{kT}{\mu A b^3}} \tag{32}$$

where A is material constant, k is Boltzmann's constant, b is magnitude of Burger's vector, $\hat{f}_{es}^0$ is saturation threshold stress at "0" K. Thermal activation function is a function of absolute temperature and strain rate and defines the ratio between the flow stress and mechanical threshold stress. This function can be obtained from the Arrhenius law with activation energies and temperature as follows:

$$f_1(\dot{\varepsilon}, T) = \left[1 - \left(\frac{kT \ln(\dot{\varepsilon}_0 / \dot{\varepsilon})}{\mu b^3 g_0} \right)^{1/q} \right]^{1/p} \tag{33}$$

where p, q are material constant, $\dot{\varepsilon}_0$ is reference strain rate, μ is shear modulus, k is Boltzmann's constant, b is magnitude of Burger's vector, g_0 is normalized activation energy.

3.2 Constitutive Relation

In order to obtain close system of constitutive equations the stress-strain relation should be defined. In a case of high velocity (shock inducing) impact the spherical part of stress tensor is described by the EOS. Using Equation (7), (13), (19), (20), (21), (25) the following relation can be written:

$$\dot{\tilde{\Sigma}} = \tilde{\tilde{C}}(\omega, \alpha) : \dot{\tilde{\varepsilon}}^e - \Lambda_1 \cdot \tilde{\tilde{C}}(\omega, \alpha) : \frac{\partial \varphi}{\partial \tilde{\Sigma}} \dot{\omega} - \Lambda_2 \cdot \tilde{\tilde{C}}(\omega, \alpha) : \frac{\partial \psi}{\partial \tilde{\Sigma}} \dot{\alpha} - \Lambda_3 \cdot \frac{\partial \zeta}{\partial \tilde{\varepsilon}^e} \dot{\Re} \tag{34}$$

$$\frac{\partial \varphi}{\partial \tilde{\Sigma}} = \left[\frac{B}{(1-\omega)(1-\alpha)} H\left(\frac{\Sigma}{(1-\omega)(1-\alpha)} - \Sigma_* \right) + \frac{\omega}{4\eta_0} H\left(\Sigma - \Sigma^+ \right) + \frac{\omega}{4\eta_0} H\left(\Sigma^- - \Sigma \right) \right] \delta_{ij} \tag{35}$$

$$\frac{\partial \psi}{\partial \tilde{\Sigma}} = \frac{C}{(1-\omega)(1-\alpha)} H\left(\frac{\Re_u}{(1-\omega)(1-\alpha)} - \Re_u^* \right) \frac{\tilde{\Re}}{\Re_u} \tag{36}$$

$$\frac{\partial \zeta}{\partial \tilde{\varepsilon}^e} = \frac{\partial}{\partial \tilde{\varepsilon}^e} \left(\Re_a + f_1(\dot{\varepsilon}, T) \cdot \hat{f} \cdot \frac{\mu_1}{\mu_0} \right) \tag{37}$$

$$\frac{\partial}{\partial \varepsilon} \left(f_1(\dot{\varepsilon}, T) \cdot \hat{f} \cdot \frac{\mu_1}{\mu_0} \right) \cdot \frac{\partial \varepsilon}{\partial \tilde{\varepsilon}^e} = f_1(\dot{\varepsilon}, T) \cdot \frac{\partial}{\partial \varepsilon} \left(\hat{f} \right) \cdot \frac{\mu_1}{\mu_0} \cdot \frac{\partial \varepsilon}{\partial \tilde{\varepsilon}^e} \tag{38}$$

$$f_1(\dot{\varepsilon}, T) \cdot \frac{\partial}{\partial \varepsilon} \left(\hat{f} \right) \cdot \frac{\mu_1}{\mu_0} \cdot \frac{\partial \varepsilon}{\partial \tilde{\varepsilon}^e} = f_1(\dot{\varepsilon}, T) \cdot \theta_0 \left[1 - F(\hat{f}_1) \right] \cdot \frac{\mu_1}{\mu_0} \cdot \frac{\partial \varepsilon}{\partial \tilde{\varepsilon}^e} \tag{39}$$

Using Equation (34), (35), (36), (39) the relation for deviatoric part of stress tensor (isotropic case) the following expression can be written:

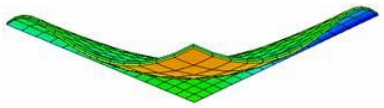

© 2004, The First International Conference on Computational Mechanics (CM'04)
Belgrade, Serbia and Montenegro, November 15-17, 2004
http://www.cm2004.matf.bg.ac.yu
Printing Faculty of Mathematics, University of Belgrade

$$\dot{\tilde{\Re}} = 2\mu(\omega,\alpha)\dot{\tilde{\varepsilon}}^{e} - \frac{\Lambda_2 \cdot C \cdot H\left(\dfrac{\Re_u}{(1-\omega)(1-\alpha)} - \Re_u^*\right)}{(1-\omega)(1-\alpha)} \frac{\tilde{\Re}}{\Re_u} \cdot \dot{\alpha} - \tag{34}$$

$$- \Lambda_3 \cdot f_1(\dot{\varepsilon},T) \cdot \theta_0 \left[1 - F(\hat{f}_1)\right] \cdot \frac{\mu_1}{\mu_0} \cdot \frac{\partial \varepsilon}{\partial \tilde{\varepsilon}^{e}} \dot{\Re}$$

4. Criteria for Fracture Initialization

The development of intensive plastic flow and accumulation of damage are processes that precede fracture. Macroscopic failure starts as formation of new free surfaces in the material − the sides of a crack. The criterion for the macroscopic failure is based on the entropy criterion for the specific critical dissipation [4]:

$$D_* = \int_0^{t_*} \frac{1}{\rho}\left(d_M + d_F + d_T\right)dt \tag{26}$$

where: t_* is the time required for the macroscopic failure to start, D_* is a material constant (critical specific entropy), d_M, d_F and d_T are mechanical dissipation, dissipation due to fracture (dissipation of continuum fracture) and thermal dissipation.

When the criterion, given in Eq. (26), is satisfied at a point in the material, a crack forms at that location. The approach used to redefine the grid and map the parameters on to the new grid is in itself an independent problem in the framework of computational mechanics [14] and is not addressed in this paper.

The proposed approach is capable of modeling tensile and compressive/shear types of failure. If material is undergoing large rapid plastic deformation then the major contribution to dissipation, Eq. (26), is made by d_M and by term $\Lambda_1\dot{\omega}^2$ in d_F. As for the development of shear plastic flow with formation of zones of adiabatic shear, the major contribution to dissipation D is made by d_M, d_T and by the term $\Lambda_2\dot{\alpha}^2$ in d_F.

4.1 Definition of Material Constants

The proposed damage model uses some non-standard constants related to damage parameters which ought to be determined.

To determine the MTS parameters a series of uniaxial tensile tests was performed in the temperature range -70ºC to 200ºC and for the strain rate range $10^{-3}s^{-1}$ to 100 s^{-1}. An example of the test data used to fit the parameters is shown in Figure 4.1.

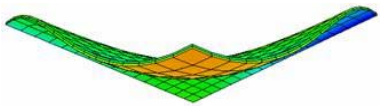

© 2004, The First International Conference on Computational Mechanics (CM'04)
Belgrade, Serbia and Montenegro, November 15-17, 2004
http://www.cm2004.matf.bg.ac.yu
Printing Faculty of Mathematics, University of Belgrade

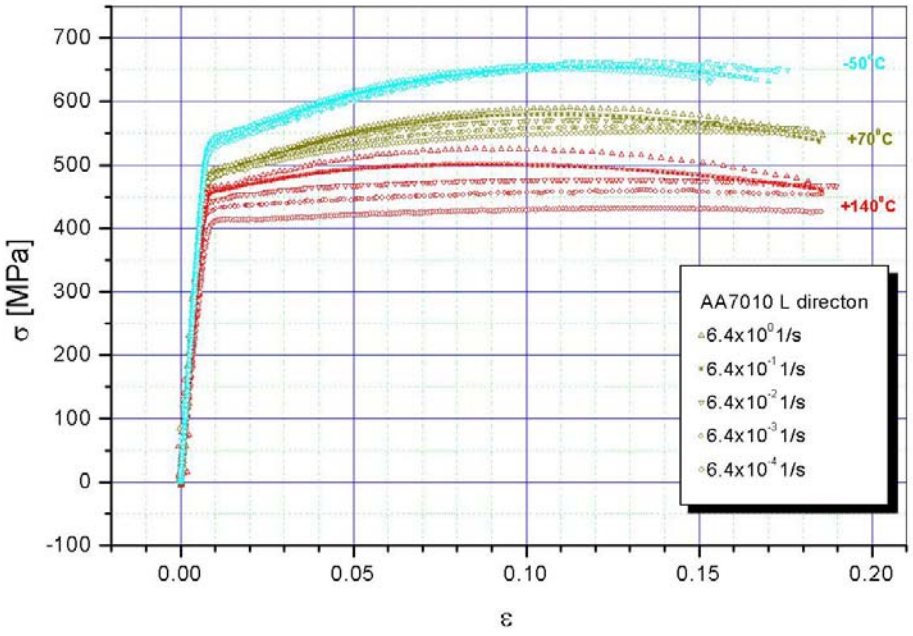

Figure 4.1 An example of tensile test data used to fit the MTS parameters for AA7010

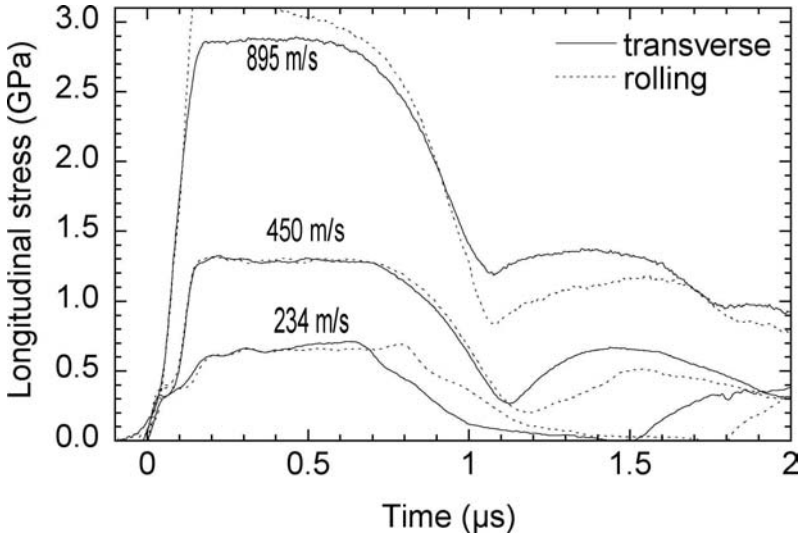

Figure 4.2 Longitudinal stress vs. time for the plate impact tests on AA 7010

The definition of the two damage parameters requires the following constants: B, C, Λ_1, Λ_2, η_0 Σ_*, $\Re_u^*$, D_* In order to determine these constants, a method based on combination of experiments and numerical modelling of the plate impact problem was used [4], [13], [14]. Note that experiments with spall failure are

nowadays the most common tool for construction of dynamic constitutive equations for materials [4,13,14].

Experimental data used to determine the material parameters is shown in Figure 4.2. It corresponds to plate impact tests for Al alloy 7010 at two velocities V=895, 450 and 234 m/s. In the tests performed at V=234 and 450 m/s no spall was observed while in the test at V=895 m/s the specimen fully spalled. The tests were performed in Cranfield's gas gun facility.

5. Validation of the Model

5.1 Taylor Test

Taylor cylinder specimens, 9.3 mm diameter with length 46.5 mm giving the length-to-diameter ratio L/D=5, were cut of from AA7010 rolled plate. A test coordinate system (axes X, Y, Z) aligned with the material coordinate system was adopted such that compressive impact loading was applied along Z-axis, see Figure 5.1.

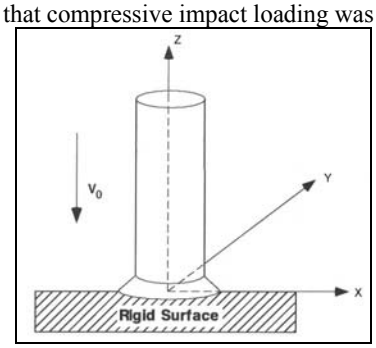

Figure 5.1 Schematic drawing of a Taylor cylinder impact test

Several Taylor tests were conducted at velocities of 200, 214, 244, 400 m/s, using a single stage gas gun.

Side View

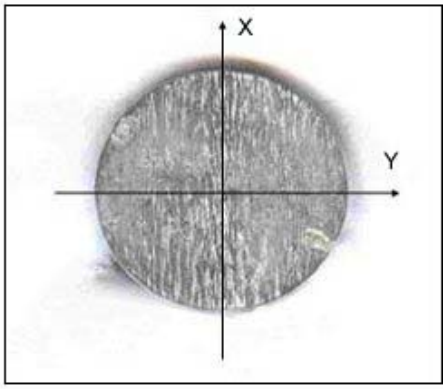

Footprint

Fig. 5.2 Photographs of the post-test geometry for the AA 7010 Taylor specimen V=200 m/s

Figures 5.2 and 5.3, present photographs of side profiles for the velocities of 200 m/s and 214 m/s, respectively, along with the footprints from a typical post-impact specimen. The observed footprints were asymmetric (elliptical) with a different level of eccentricity.

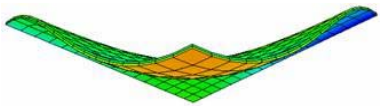

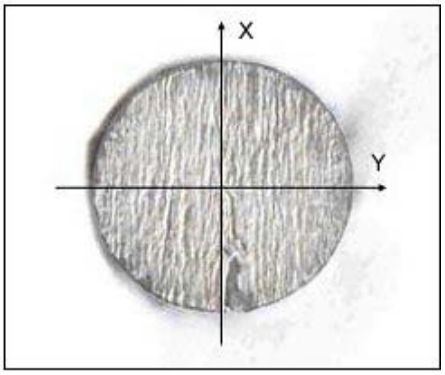

Side view Footprint

Fig. 5.3. Photographs of the post-test geometry for the AA 7010 Taylor specimen V=214 m/s

Tests were performed at velocities 244, 400 m/s resulted in failure dominated by shear and were not of direct relevance to the work presented in the paper.

Geometries for the deformed specimens were digitised using a 3D scanning machine. The geometrical data of specific interest was side profiles for minor and major axis. Final specimen heights are: 42.2 mm for specimen impacted at 200 m/s, and 42.1 mm for specimen impacted at 214 m/s. Eccentricity (ratio of major to minor diameters) for the specimen impacted at 200 m/s was 1.04, and eccentricity for specimen impacted at 214 m/s was 1.06. Figure 5.4 shows comparison of minor and major side profiles of post-test geometry plotted as radial strain vs. distance.

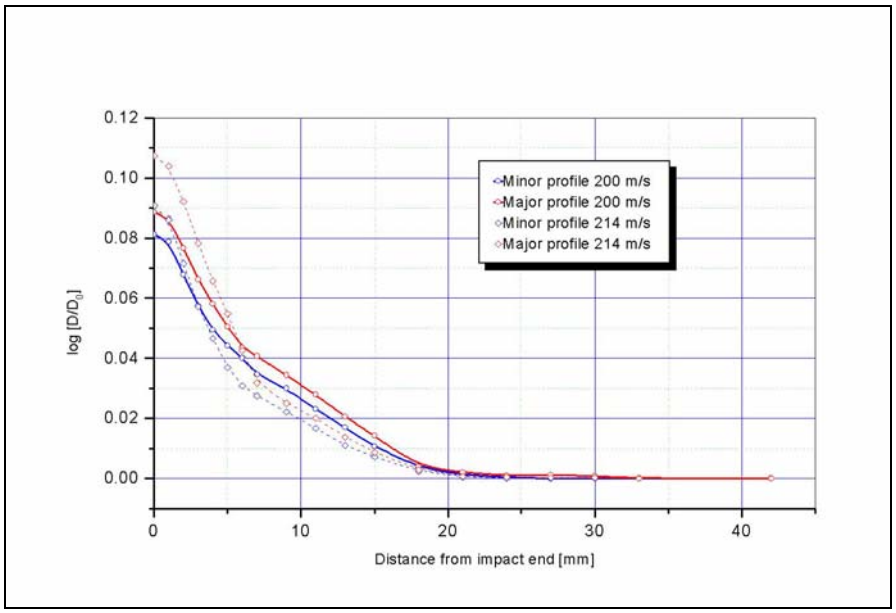

Fig. 5.4. Comparisons of the major and minor axis profiles of post-test geometry for the AA 7010 Taylor specimens impacted at 200 and 214 m/s plotted as radial strain vs. distance

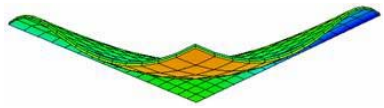

© 2004, The First International Conference on Computational Mechanics (CM'04)
Belgrade, Serbia and Montenegro, November 15-17, 2004
http://www.cm2004.matf.bg.ac.yu
Printing Faculty of Mathematics, University of Belgrade

5.2 Taylor test simulation

In order to analyse proposed model for tensile failure, it was implemented in DYNA3D code and incorporated into MTS material model. The strength material model was used in the combination with a Gruneisen Equation of State. The material parameters of the Gruneisen Equation of State for AA 7010 are summarized in the Table 5.1. A series of FE simulations of Taylor cylinder impact test were performed for AA7010. In the simulations the $cm-g-\mu s$ system of units was used.

Table 5.1. Grunisen EOS constants

Parameter	Description	Nominal value
C_0	Bulk sound speed	0.5386 $cm/\mu s$
S_1	First Hugoniot slope coefficient	1.339
S_2	Second Hugoniot slope coefficient	0
S_3	Third Hugoniot slope coefficient	0
γ_0	Gruneisen coefficient	1.97
B	First order volume correction coefficient	0.48
E_0	Initial internal energy	0.0
V_0	Initial relative volume	1.0

On the basis of published data for spall strength for aluminium alloy AA 7020 [17] (Figure 5.5), parameters, which are included in proposed failure criterion, were determined as: threshold stress $\sigma_0 = 1.05GPa$, normalized activation energy $u_0 = 0.0087$ and critical time $t_{c0} = 2\mu s$.

Values of the other parameters, which are included in the proposed criterion are: Boltzmann's constant $k = 1.38X10^{-23}\,J/K$, Burger's vector $b = 0.286X10^{-9}\,m$, and

Shear modulus $\mu = b_0 - \dfrac{b_1}{\exp(\frac{b_2}{T}) - 1}$, where $b_0 = 28.83GPa$ is shear modulus at 0K, and $b_1 = 4.45GPa$, $b_2 = 248.5K$.

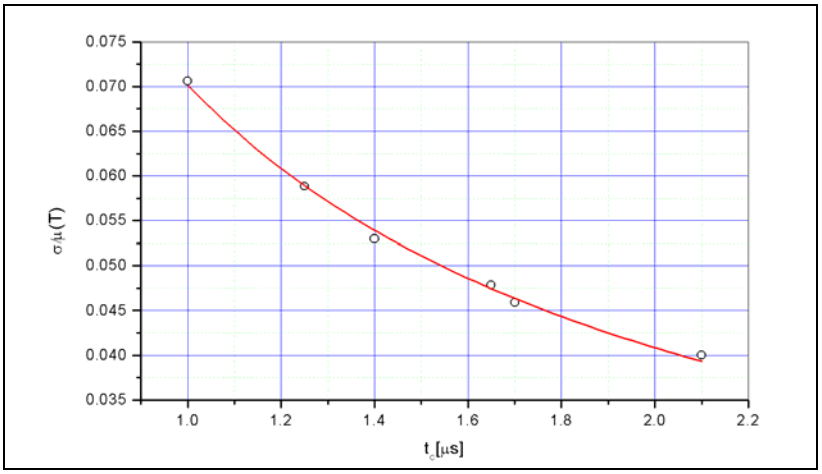

Figure 5.5. Normalized critical spall stress versus critical time of loading for AA7020

In order to reduce the number of elements in the simulations model, and the overall time of simulations, only quarter of Taylor cylinder was modelled with a uniform solid butterfly mesh.

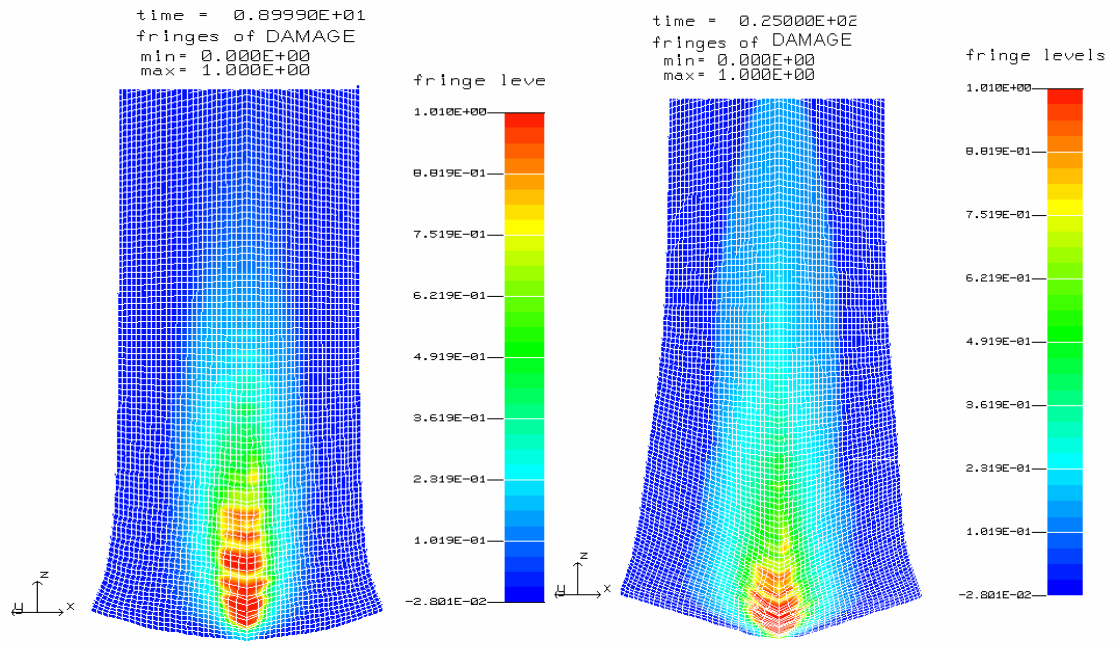

V=214 m/s

Figure 5.6. Damage distribution at response time t=9 μs and t= 25 μs in AA7010 Taylor specimen for impact velocity V=200 m/s

Damage generated in Taylor specimen for impact velocity of 200 m/s at two different response times is shown in Figure 5.6. Loading that material is exposed to generates tensile stresses in materials, leading to damage and fracture, if the amplitude and duration of the loading are sufficient. This computer simulation showed that reflected compressive and lateral release waves interacting in the specimen, generated tensile stresses high enough to cause development of damage and fracture. The damage is distributed in the region around the axis of the cylinder close to the impact surface. The voids that developed and coalesced in the initial stage of the impact were compressed at the later stages of the cylinder deformation process (see Figure 5.6).

Implemented damage model initiates damage if the mean stress become more tensile then the specific limit, threshold stress. Once initiated, damage evolves according to the proposed cumulative law and when the criterion for macroscopic failure is reached the elements fails and is removed from calculation.

Comparisons of simulated Taylor cylinder profile with minor and major side profiles of post-test geometry for Taylor specimens impacted at 200 m/s and 214 m/s are presented in Fig. 5.7 and Fig. 5.8.

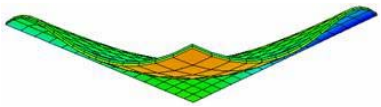

© 2004, The First International Conference on Computational Mechanics (CM'04)
Belgrade, Serbia and Montenegro, November 15-17, 2004
http://www.cm2004.matf.bg.ac.yu
Printing Faculty of Mathematics, University of Belgrade

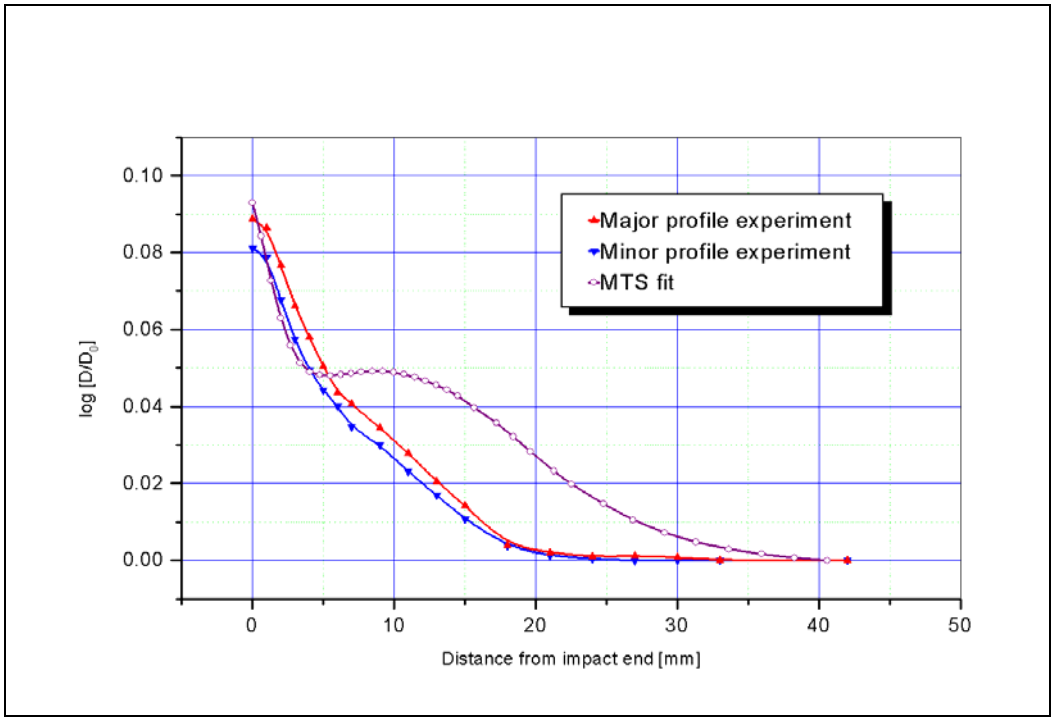

Fig. 5.7. Major and minor side profile of post-test geometry and simulation results for the AA 7010 Taylor specimen impacted at 200 m/s plotted as radial strain vs. distance

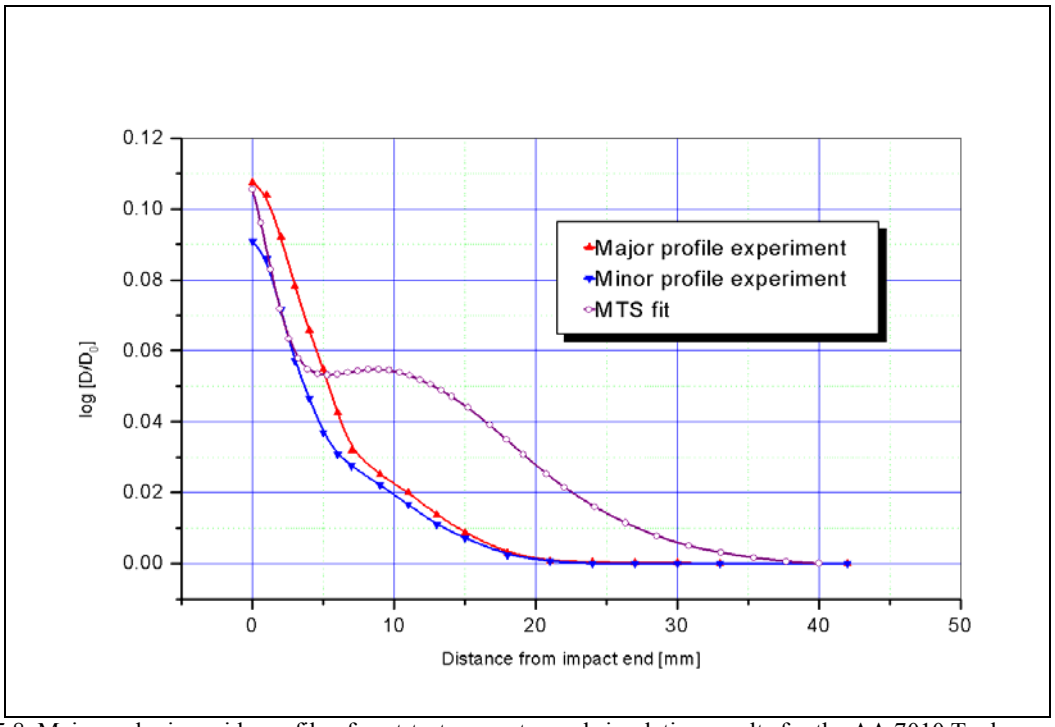

Fig. 5.8. Major and minor side profile of post-test geometry and simulation results for the AA 7010 Taylor specimen impacted at 214 m/s plotted as radial strain vs. distance

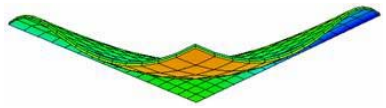

6. Summary

Parameters for constitutive relations were derived on the basis of tensile and plate impact tests, and used as input parameters for numerical simulation of Taylor impact test for AA7010.
Comparing the experimental with DYNA3D simulation results, which incorporated the proposed damage model with MTS constitutive model, the following conclusions can be made.
Simulations clearly show, that proposed damage/failure model, based on the assumption that fracture process occurs with assistance of thermal activation processes, together with MTS constitutive relation, can simulate high strain rate deformation processes and dynamic failure in tension.
The MTS flow stress model needs to be carefully characterized for the material of interest within strain, strain rate and temperature regime to obtain accurate calculation results, in this case capturing the cylinder specimen heights, and axial major and minor distributions of plastic strain.
Proper validation of the damage model will be done when analysis of damage in the test specimens is completed.

References

[1] A. A. Ilyushin (1967), On Some Theory of Long Strength, Mech. Solids, 2(3), 21-35.
[2] L. M. Kachanov (1958), On Destruction in Creeping of Materials, Izv. Acad. Nauk USSR, Section of Eng. Sci., 22(8), 26-31.
[3] Yu. N. Rabotnov (1959), Mechanism of Long Fracture, Problems of strength of materials and constructions, Moscow, USSR Academy of Sci. Publ., 5-7.
[4] A. B. Kiselev, A. A. Lukyanov (2002), Mathematical Modeling of Dynamic Processes of Irreversible Deforming, Micro- and Macro-fracture of solids and structures, Int. J. of Forming Processes, 5(2-3-4), 351-362.
[5] A. A. Lukyanov (2004), Prediction of failure in metal structures based on thermodynamics of irreversible process, Proceeding IPC 2004, ASME.
[6] B. Luccioni, S. Oller (2003), A Direction Damage Model, Comput. Methods Appl. Mech. Engrg., 192, 1119-1145.
[7] M. Brunig (2003), Numerical Analysis of Anisotropic Ductile Continuum Damage, Comput. Methods Appl. Mech. Engrg., 192, 2949-2976.
[8] B. D. Coleman, H. E. Gurtin, 1967, Thermodynamics with Internal State Variables, J. Chem. Phys., 47(2), 597-613.
[9] F. R. Tuler, B. M. Butcher, A criterion the time dependence of dynamic fracture, The international journal of fracture mechanics (1968), 4(4), 431-437.
[10] Steinberg, D.J. and M.W. Guinan, "A High-Strain-Rate Constitutive Model for Metals, "University of California, Lawrence Livermore National Laboratory, Rept. UCRL-80465, 1978.
[11] T. W. Wright (2002), The Physics and Mathematics of Adiabatic Shear Bands, Cambridge University Press.
[12] D. M. Goto, J. Bingert, S. R. Chen, G. T. Gray, III and R. K. Garrett (2000), The Mechanical Threshold Stress Constitutive Strength Model Description of HY-100 Steel, Metallurgical and Material Transactions A, 31(8), 1985-1996.
[13] S. Hanim, J. R. Klapaczko (1999), Numerical study of spalling in an aluminium alloy 7020-T6, International journal of Impact Engineering, 22, 649-673.
[14] G. I. Kanel, S. V. Razorenov, A. Bogatch, A. V. Utkin, V. E. Fortov, Spall fracture properties of aluminum and magnesium at high temperatures, J. Appl. Phys. 1996; 79 (11), 8310–8316.
[15] R. Vignjevic, N. K. Bourne, J. C. F. Millet, T. De Vuyst, Effects of orientation on the strength of the aluminium 7010-T6 during shock loading: Experiment and simulation, J. Applied Physics, 92(8), 4342-4348.
[16] L. I. Sedov (1972), A Course in Continuum Mechanics, Wolters-Noordhoff Publishing, Groningen.